

Characteristics and complete genome analysis of pathogenic *Aeromonas veronii* from diseased *Siniperca chuatsi*

Xinhai Zhu

Yangzhou University

Lijie Qin

Yangzhou University

Yujie Zhu

Yangzhou University

Qieqi Qian

Yangzhou University

Xiaojian Gao

Yangzhou University

Qun Jiang

Yangzhou University

Jun Wang

Yangzhou University

Guoxing Liu

Freshwater Fisheries Research Institute of Jiangsu Province

Xiaojun Zhang (✉ zxj9307@163.com)

Yangzhou University

Research Article

Keywords: *Aeromonas veronii*, *Siniperca chuatsi*, pathogenesis, resistance mechanism, complete genome

Posted Date: August 10th, 2023

DOI: <https://doi.org/10.21203/rs.3.rs-3217025/v1>

License:   This work is licensed under a Creative Commons Attribution 4.0 International License.

[Read Full License](#)

Additional Declarations: No competing interests reported.

Version of Record: A version of this preprint was published at Marine Biotechnology on November 10th, 2023. See the published version at <https://doi.org/10.1007/s10126-023-10253-0>.

Abstract

As an opportunistic pathogen, *Aeromonas veronii* can cause hemorrhagic septicemia of various aquatic animals. In our present study, a dominant strain SJ4 isolated from naturally infected mandarin fish (*Siniperca chuatsi*), was identified as *A. veronii* according to the morphological, physiological, and biochemical features, as well as molecular identification. Intraperitoneal injection of *A. veronii* SJ4 into *S. chuatsi* fingerlings revealed clinical signs similar to the natural infection, and the median lethal dosage (LD₅₀) of the SJ4 to *S. chuatsi* was 3.8×10^5 CFU/mL. Histopathological analysis revealed that the isolate SJ4 could cause cell enlargement, obvious hemorrhage and inflammatory responses in *S. chuatsi*. Detection of virulence genes showed the isolate SJ4 carried *act*, *fim*, *flgM*, *ompA*, *lip*, *hly*, *aer*, *eprCAL* and the isolate SJ4 also produce caseinase, dnase, gelatinase, and hemolysin. In addition, the complete genome of *A. veronii* SJ4 was sequenced, and the size of the genome of *A. veronii* SJ4 was 4562694 bp, within a G + C content of 58.95%, containing 4079 coding genes. 910 genes encoding for several virulence factors such as type III and VI secretion system, flagella, motility, *etc.*, were determined based on the VFDB database. Besides, 148 antibiotic resistance-related genes in 27 categories related to tetracyclines, fluoroquinolones, aminoglycosides, macrolides, chloramphenicol, and cephalosporins were also annotated. The present results suggested that *A. veronii* was etiological agent causing the bacterial septicemia of *S. chuatsi* in this time, as well as provided a valuable base for revealing pathogenesis and resistance mechanism of *A. veronii*.

1. Introduction

Siniperca chuatsi is one of the most economically important freshwater fish species in China, and has a high market value due to fast growth, high nutrition and low fat (Shen et al. 2021). The scale expansion of the mandarin fish industry has resulted in a high annual production of 373.9 thousand tons according to China Fishery Statistical Yearbook in 2021. Recently, aquaculture has become highly sensitive to frequent pathogenic infections because of the high-density culture and the deterioration of water environment, which seriously threaten the steadiness and development of the fishery industry, and the bacterial infections percentage has risen to about 25% in freshwater fish disease outbreaks (Tyagi et al. 2022). In recent years, various bacterial pathogens were frequently increasing and causing highly troublesome losses to *S. chuatsi* industry, including *Flavobacterium columnare*, *Aeromonas hydrophila*, *Gytophaga columnaris*, *Streptococcus uberis*, *Aeromonas salmonicida*, *etc* (Chen et al. 1995; Zhou et al. 2015; Luo et al. 2017; Chen et al. 2018; Lin et al. 2020). In this study, mass mortalities of *S. chuatsi* with bacterial septicemia occurred in Yangzhou, Jiangsu Province China, and *A. veronii* was identified as the primary pathogen for the hemorrhagic septicemia in *S. chuatsi*.

A. veronii, a gram-negative, rod-shaped, facultative anaerobic bacterium, has a strong adaptability to the environment and is widely distributed, especially freshwater areas and estuaries (Tekedar et al. 2019). Among various bacterial pathogens, mesophilic *Aeromonas* species (*A. veronii*, *A. hydrophila*, *Aeromonas sobria*, *etc*), causing motile *Aeromonas* septicemia (hemorrhagic septicemia), has often been reported as the major cause of fish mortalities around the globe (Janda and Abbott 2010; Mishra et al. 2017). In

recent years, *A. veronii* has been recognized as an aquatic pathogen to various fish species, such as *Ictalurus punctatus*, *Oreochromis niloticus*, *Dicentrarchus labrax*, *Misgurnus anguillicaudatus*, *Carassius auratus*, *Labeo rohita*, *Odontobutis potamophila*, *Silurus asotus*, *Astronotus ocellatus*, etc (Huang et al. 2010; Sreedharan et al. 2011; Kim et al. 2013; Dong et al. 2017; Smyrli et al. 2017; Kaur et al. 2020; Shameena et al. 2020; Zhang et al. 2020; Liu et al. 2022). It is visible that the cases of economic loss and water environment pollution in aquaculture caused by the spread of *A. veronii* was rapidly increasing. Therefore, more attention should be attracted to the widespread infections and virulence mechanisms of *A. veronii* in aquatic animals.

As is well-known, the bacterial pathogenicity was based on many virulence-related factors, such as colonization, invasiveness, exotoxins, endotoxins, and extracellular enzymes etc (Tyagi et al. 2022). These virulence-related factors help the pathogen to colonize, invade and attack the host, immune escape, proliferate and cause disease (Sharma et al. 2017). Relative to single action, multiple virulence factors work synergistically, which is more beneficial for bacterial invasion (Haslinger *et al.* 2005). Thus, the genes encoding for virulence factors have often been used to determine the potential pathogenicity of bacterial pathogens (NAILIS *et al.* 2005). Now, with the update of NGS technologies and the development of utility tools, it has become more feasible to investigate whole genomes of various bacterial pathogen with high speed and accuracy. Thus, the WGS technology would play a crucial role into species identification, gene function annotation, genome structure difference analysis of various pathogens (Donkor 2013).

In the present study, *A. veronii* SJ4 was isolated from the kidneys of diseased *S. chuatsi*, and the pathogenicity of SJ4 was confirmedly determined by experimental infection, histopathology changes and virulence gene examination. Additionally, the complete genome of *A. veronii* SJ4 was sequenced, and the virulence-related genes and antibiotic resistance genes were analyzed for revealing pathogenesis and resistance mechanism of *A. veronii* SJ4. The present results suggested that *A. veronii* was etiological agent causing the bacterial septicemia in *S. chuatsi* aquaculture of this time, and the whole genome sequencing analysis provided a better understanding of the pathogenesis and resistance mechanism of *A. veronii*.

2. Materials and Methods

2.1 Fish disease and bacterial isolation

The diseased moribund *S. chuatsi* were collected from the aquaculture farm in Yangzhou, Jiangsu Province, China. The samples were examined for external clinical signs, and aseptically dissected after sterilization of body surface with 75% ethanol. The livers, gills, kidneys, and spleens samples were inoculated and streaked separately onto LB agar plates, which were cultured for 12h at 28°C. The dominant single colony were re-streaking on the LB agar tube, and the bacteria were stored in LB medium with 30% glycerol at -80°C for further study.

2.2 Bacterial virulence assay

The representative dominant strain SJ4 was selected and incubated in LB medium at microbiological incubator (180 rpm, 28°C) for 18 h, and the bacterial fluid was suspended with sterile PBS (pH 7.4) to the concentrations from 2.4×10^8 to 2.4×10^5 CFU/mL. Twenty *S. chuatsi* (100–120 g) confirmed to be free of pathogen infection in each tank, were injected intraperitoneally with 100 μ L bacteria within different concentration (2.4×10^8 , 2.4×10^7 , 2.4×10^6 , 2.4×10^5 CFU/mL) per fish, respectively. In the control group, sterile PBS was injected intraperitoneally in each fish. The survival situation of each fish was monitored daily for 14 d, and the cumulative mortalities of experimental fish were recorded to calculate the LD₅₀ of *A. veronii* to *S. chuatsi* by using methods of Behrens and Karber (1953).

2.3 Histopathology

The tissue samples of livers, spleens, kidneys and gills were fixed in 10% neutral buffered formalin. The formalin-fixed tissues were dehydrated in ethanol and embedded in paraffin wax blocks, which sectioned at 6 μ m and H&E-stained for optical microscope observation.

2.4. Morphology Observation

The pure cultured SJ4 cells were collected by centrifuge at 6000g, 4°C for 10 min and washed thrice with sterile PBS. Then the bacteria cells were cooled at 4°C with glutaraldehyde (0.25 g/L), post-fixed with osmium tetroxide in 0.1 M cacodylate buffer, and adhered onto Poly-L-Lysine coated coverslips. Then the graded ethanol was used for dehydration and the gold palladium alloy was coated on EMS (Electron Microscopy Science). Finally, the Zeiss EM10 was used for the observation of the flagella cells, the types and sizes of which would be analyzed.

2.5. Identification of bacterial isolates

33 kinds of the biochemical reaction tubes (Hangzhou Binhe Microorganism Reagent Co., Ltd., China) were selected for the biochemical tests, including Gram staining, Oxidase, Voges–Proskauer, Indole production, Sucrose, Maltose, Raffinose, Lactose, Melibiose, Cellobiose, Galactose, Glucose, Mannitol, Arabitol, *etc.* The results of the tests would be compared with the description in Bergey's Manual of Systematic Bacteriology (Brenner et al. 2021).

The 16S rRNA and *gyrB* genes of SJ4 were PCR amplified with primers as per previously described protocols of Zhang et al. (2014). After sequencing in Shanghai Sangon Biotech Co., Ltd., it is searched in NCBI of the 16S rRNA and *gyrB* sequences of isolate SJ4 to analyze sequence homology by using the BLAST. The maximum likelihood method was adopted to construct the phylogenetic trees using MEGA 7.0 (Kumar et al. 2016).

2.6 Determination of extracellular enzymes and hemolysin

The extracellular enzymatic activities including phospholipase, lipase, amylase, hemolysin, urease, caseinase, dnase, and gelatinase, were screened by the methods described by Gao et al. (2020). LB agar plates were supplemented with 10% egg yolk, 1% Tween-80, 2% starch, 7% rabbit erythrocytes, 2% urea, 10% skim milk, 0.05% DNA, 1% gelatin, respectively. 5 μ l bacteria suspension was spot-inoculated onto

the center of plates, which were cultured at 37°C for 18h with triplicates. If the isolate SJ4 possesses the corresponding extracellular enzyme activities, the colonies would surround a circle of lytic halo.

2.7 Detection of virulence related genes

The polymerase chain reaction was performed using Easy Taq PCR Super® Mix (Tolo Biotech Co., Ltd) to detect the presence of virulence-related genes in the isolate SJ4, including *act*, *fim*, *flgM*, *ompA*, *Lip*, *hly*, *aer*, and *EprCAI*. The specific primers were designed according to the genome data (Table 1). The length of PCR productions was estimated by 1% Agarose gel electrophoresis.

Table 1
The primers used for the PCR.

Gene	Primer sequences (5'-3')	Product length (bp)
<i>act</i>	AGAAGGTGACCACCAAGAACA AAGTACTGACATCGGCCTTGA	232
<i>fim</i>	TGCCCGTTCGCCTCTTTA GGCTTCGGTCTTGCCATT	110
<i>flgM</i>	GCTACTGTCAAGCTGGACTC AGATTGGCCTCGAACTG	194
<i>ompA</i>	GCGGTTTATCGCTTTGGT CACGCTTGGACTTGCTGA	397
<i>lip</i>	GTGCCGTCTGCCTTGGTGA CCCGTCTATTGCGGGTTCGA	598
<i>hly</i>	CGGACGATTATCAGGATGG CAAGAACGAGTTTCAGTGGC	289
<i>aer</i>	CCTATGGCCTGAGCGAGAAG CCAGTTCCAGTCCCACCACT	417
<i>EprCAI</i>	GCTCGACGCCAGCTCACC GGCTCACCGCATTGGATTTCG	387

2.8 Whole-genome sequencing and assembly

For next-generation sequencing (NGS), SJ4 bacterial genomic DNA isolation kit (TransGen Biotech Co., Beijing) was used to extract the genomic DNA from the overnight grown culture of *A. veronii* SJ4. Agarose gel electrophoresis was also used to check the quality of genomic DNA. The whole genome of SJ4 was sequenced by the third-generation PacBio RS II combined with the second-generation Illumina HiSeq2000

sequencing method, which was completed by Shanghai OE Biotech Co., Ltd. Qualified DNA samples were sequenced using PacBio RS II single-molecule real-time (SMRT) sequencing technology (Pacific Biosciences, Menlo Park, CA, USA) to have their entire genome sequenced. Then the hierarchical genome-assembly process (HGAP) was used to assemble randomly interrupted sequence read segments to obtain very long sequence read segments. Next, the second-generation sequencing technology Illumina HiSeq 2000 was used for sequencing, and Bowtie2 (v2.3.0) was used to compare the Illumina gene fragments with the assembled SMRT-contigs, so as to obtain the complete circular whole genome sequence information. Glimmer 3.02 was used for gene prediction and annotation, tRNAscan-SE was used for prediction and screening of tRNA genes, RNAmmer software was used for prediction and analysis of rRNA, and Rfam (v10.0) was used for prediction and screening of sRNA. Subsequently, RepeatMasker (v4.0.7) software was used to predict the tandem repeat and interspersed repeat.

2.9 Genome annotation and comparative genomics

In terms of database annotations, several are commonly used, such as NR annotation, COG/KOG functional annotation, GO classification, Swissprot, eggNOG, KEGG, and Pfam. DIAMOND software was employed for comparison of NR, COG/KOG, GO, Swissprot, eggNOG, and KEGG database annotations, and annotations with $e < 1e-5$ were obtained by selecting proteins that possess the highest sequence similarity. The Pfam database comprises a compilation of protein families, each represented by multiple sequence alignments and hidden Markov models. HMMER software was utilized to compare protein family models, and the family with the highest score was chosen. Moreover, blast was used to compare with the CARD resistance gene database, and annotations with $e < 1e-10$ were chosen. The VFDB database is specifically designed for studying the pathogenic factors of pathogenic bacteria, chlamydia, and mycoplasma. Annotations with $e < 1e-10$ were selected via comparison with the VFDB database using DIAMOND software.

3. Results

3.1 Pathological Symptoms of diseased fish and bacterial isolation

According to the epidemiological investigation, the diseased *S. chuatsi* exhibited multiple symptoms including gill pallor, muscle bleeding and necrosis, fin erosion, as well as abdominal enlargement, redness and swelling (Fig. 1). Anatomical examination revealed that internal organ damage caused the accumulation of yellow or red ascites in the abdominal cavity and led to organ enlargement, specifically in the liver, spleen, and kidney. Abundant pure bacteria isolated from the livers, spleens, kidneys, and gills of the diseased *S. chuatsi*, and these colonies exhibited the characteristics of white, translucency, circle, convex, glaze surface and intact edge. A representative strain from these was selected for this study, which was tentatively named SJ4.

3.2 Virulence of the isolate

The results of bacterial virulence assay were shown in Fig. 2. The *S. chuatsi* of experimental group started death from first day. The 2.4×10^8 , 2.4×10^7 , 2.4×10^6 , 2.4×10^5 , 2.4×10^4 CFU/ mL of SJ4 caused 100%, 100%, 70%, 50%, 10% mortalities after 14 dpi, respectively, while all fish of control group were still alive. The calculated LD₅₀ of SJ4 to *S. chuatsi* was 3.8×10^5 CFU/mL. Furthermore, the isolate SJ4 was re-isolated from the infected *S. chuatsi*, confirming that this experiment satisfies Koch's postulates.

3.3 Histological observation

Compared to the control group, the liver tissues of the experimental group presented with swelling, hemorrhage, necrosis, and interstitial hyperplasia among liver cells (Fig. 3B). Similarly, the respiratory epithelial cells of the secondary gill plate exhibited clear signs of necrosis with the bended branchial lamellae, while the epithelial cells exhibit proliferate and necrosis (Fig. 3D). Furthermore, the spleen tissues of the experimental group showed distinct manifestations of telangiectasia, hyperemia, hemolysis, and blood spot formation, with severe regional rupture (Fig. 3F). The focal area of the kidney displayed symptoms of loss of brush border, glomerular necrosis, and necrotic interrenal tissue cells with chapped morphology (Fig. 3H).

3.5. Electron Microscopic Observation of the Isolate

The isolate SJ4 exhibited single polar flagellum and a shape of rod-shaped with round-ends, about 1.4–2.1 μm wide and 2.8–5.3 μm long, upon the electron microscopic observation (Fig. 4).

3.6 Physiological and biochemical characterization

By physiological and biochemical observation, the isolate SJ4 showed similar characteristics of *A. veronii* bv *veronii* as the description in Bergey's Manual of Systematic Bacteriology. As shown in Table 2, oxidase, Voges–Proskauer, Indole production, Fructose, Cellobiose, and β -galactosidase were produced, but not Raffinose, Lactose, Xylose, Arabitol, Tartrate, Acetate. The Sorbitol, Amygdalin and Rhamnose of the isolate SJ4 showed positive activity, which exhibits different characteristics with *A. veronii* bv *veronii* described in Bergey's Manual of Systematic Bacteriology.

Table 2
Physiological and biochemical characteristics of strain SJ4.

Characteristics	SJ4	<i>A. veronii</i>	<i>A. veronii</i>
		<i>bv sobria</i> *	<i>bv veronii</i> *
Gram staining	-	-	-
Oxidase	+	NT	NT
Voges-Proskauer	+	-	+
Indole production	+	-	+
Sucrose	+	+	+
Maltose	+	+	+
Raffinose	-	V	-
Lactose	-	V	V
Xylose	-	NT	NT
Mannose	+	+	+
Fructose	+	NT	NT
Melibiose	-	-	-
Cellobiose	+	-	V
Galactose	+	NT	NT
Glucose	+	+	+
Mannitol	+	+	+
Arabitol	-	NT	NT
Sorbitol	+	-	-
0%NaCl	+	+	+
1%NaCl	+	+	+
2%NaCl	+	+	+
6%NaCl	-	NT	NT
Tartrate	-	NT	NT

Note: "+", positive; "-", negative; D, 11 89% positive with incubation at 35°C for 7 d except for *A. veronii*, which were incubated at 25°C. "*" the data of *A. veronii* come from Bergey's Manual of Systematic Bacteriology.

Characteristics	SJ4	<i>A. veronii</i>	<i>A. veronii</i>
		<i>bv sobria</i> *	<i>bv veronii</i> *
Amygdalin	+	-	-
Acetate	-	NT	NT
β -galactosidase	+	D	+
Catalase	+	+	+
Trehalose	+	+	+
α -Methyl-d-glucoside	+	+	+
Dulcitol	-	-	-
Erythritol	-	-	-
Rhamnose	+	-	-
Motility	+	+	+

Note: "+", positive; "-", negative; D, 11 89% positive with incubation at 35°C for 7 d except for *A. veronii*, which were incubated at 25°C. "*" the data of *A. veronii* come from Bergey's Manual of Systematic Bacteriology.

3.7 Molecular identification

The 16S rRNA gene and gyrase submit B gene of SJ4 were sequenced by Sengon Biotech and assembled by Seqman after PCR. The 16S rRNA sequences of isolate SJ4 showed 99% sequence identities with *A. veronii* isolates in the NCBI Reference RNA Sequences (refseq rna) database (accession number: OQ826708), and the phylogenetic tree showed the isolate SJ4 belong to *A. veronii* (Fig. 5A). Besides, the gyrB sequences showed 98% sequence identities with *A. veronii* isolates in the NCBI Reference RNA Sequences (refseq rna) database (accession number: OQ845908), and the phylogenetic tree also showed the isolate SJ4 belong to *A. veronii* (Fig. 5B).

3.8 Virulence factors of the pathogenic isolate

The cytolytic enterotoxin (*act*), flagellin (*fim*, *flgM*), outer membrane protein A (*ompA*), Lipid A acyltransferase (*Lip*), hemolysin (*hly*), aerolysin (*aer*), Epsilon proteobacterial Calcium-binding Autotransporter-like protein (*eprCAL*) were detected by PCR detection. The extracellular enzymes activities of SJ4 were shown in Fig. 6. The strain SJ4 could produce caseinase, dnase, gelatinase, and hemolysin activity.

3.9 Genome structure and general features of *A. veronii* SJ4 genome

The genome of *A. veronii* strain SJ4 was sequenced using Nanopore, and the genome characteristics are also summarized. The genome size of SJ4 was determined to be 4562694 bp with a GC content of 58.95%. A total of 4079 coding genes were identified, with a combined length of 3973236 bp. In addition, 229 simple repetitive sequences were found, totaling 10430 bp and representing 0.23% of the genome size. as shown in Fig. 7, the genome also contained 124 tRNA genes, 43 sRNA genes, and 31 rRNA genes.

3.10 COG Analysis

The protein-coding genes with biological functions in the genome of experimental strain SJ4 were annotated by comparing them with the COG database. Based on the COG classification standards, these genes were categorized into 25 classes represented by uppercase English letters (A-Z), and a homologous gene annotation was performed. A total of 3271 protein-coding genes were annotated. As shown in Fig. 8, the annotation results for the basic function prediction genes were the most abundant, with 456 genes accounting for 13.94% of the annotated genes. The next most abundant category was amino acid transport and metabolism, with 371 genes accounting for 11.34% of the annotated genes. Signal transduction mechanisms (287 genes; 8.77%), transcription (284 genes; 8.68%), and energy production and conversion (240 genes; 7.34%) were also well-annotated. In addition, 299 genes (9.14%) with unknown functions require further investigation in future studies.

3.11 GO Analysis

The protein sequences of the predicted genes were compared with the GO database by BLASTp to obtain GO annotation information. The DIAMOND software was used for comparison, and proteins with the highest sequence similarity were selected for GO functional clustering analysis. A total of 2945 protein-coding genes were successfully annotated with GO functions. The GO annotation includes three aspects: Biological processes, Cellular components, and Molecular functions. As shown in Fig. 9, in terms of biological processes, the annotated genes were mainly related to cellular processes, metabolic processes, and localization. In terms of cellular components, the annotated genes were mainly related to cells, cell parts, and membranes. In terms of molecular functions, the annotated genes were mainly related to catalytic activity, binding, and transporter activity.

3.12 KEGG Analysis

The Kyoto Encyclopedia of Genes and Genomes (KEGG) is a database that annotates genes, genomes, and metabolic pathways at the molecular level. In this study, we compared the genome of *Vibrio* sp. SJ4 with the KEGG database and found that 2461 genes could be mapped to 165 metabolic pathways, accounting for 60.33% of all genes. As shown in Fig. 10, the metabolic pathway-related genes could be classified into 29 categories and 5 major classes, namely, cellular processes, environmental information processing, genetic information processing, metabolism, and organismal systems. KEGG enrichment analysis revealed that the strain was mostly involved in metabolism pathways, followed by environmental information processing.

3.13 Prediction of Virulence Genes of the Strains SJ4

By comparison using the virulence factor database (VFDB), it was found that there are 910 coding sequences that may be virulence genes in the whole genome of the pre-test strain SJ4. Among them, most of the genes are related to secretion systems, toxins, two-component systems, superoxide dismutase, etc. (Table 3). The experimental strain SJ4 has type III and type VI secretion systems, and the effector factors *lpg* (gene0212, gene1207, gene1209, gene1211) of the Dot/Icm type IV secretion system, the effector factor *LirB* (gene3402) of the type IV secretion system, the ABC transporter protein gene *Pmen_2312* (gene1763), and other genes are involved in the formation and regulation of the type IV secretion system, while the effector factor *VPA0450* (gene1674), the ATPase *hrcN* (gene2447), *ssaN* (gene2488), and other genes are involved in the formation and regulation of the type III secretion system. Genes such as the exfoliative toxin gene *eta* (gene0151), the toxin co-regulated pilus biogenesis protein gene *tcpI* (gene0280, gene0886, gene1105, gene2909), the structural toxin protein gene *rtxA* (gene0808), the aerosol toxin gene *aerA* (gene2830), and the enterotoxin gene *act* (gene2830) are related to the virulence of bacteria. The encoded proteins are important proteins involved in carbohydrate and amino acid metabolism and also have a certain impact on the expression of bacterial flagella and pili.

Table 3
The annotation of virulence factors of the strain SJ4 in VFDB databases.

Virulence Factors Description	Number	genes
Polar flagella	73	flmH, pomB2, nueB, flaJ, cheW, fliA, flhG, etc.
Tap type IV pili	22	tapF, tapW, tapQ, tapP, tapO, tapN, tapM, etc.
direct heme uptake system	13	hutA, hutZ, hutX, hutB, hutC, hutD, etc.
Heme biosynthesis	14	hemH, hemL, hemA, hemM, hemE, etc.
Type I fimbriae	5	fimF, fimE, fimD, fimC, fimA
T2SS	15	tapD, exeN, exeM, exeL, exeK, exeJ, exeI, etc.
Mannose-sensitive hemagglutinin (Msh) pilus	15	mshI, mshI1, mshJ, mshK, mshL, mshM, mshN, etc.
Flp type IV pili	13	flp1, flpA ~ L.
Hemolysin III	1	B565_0799
Thermostable hemolysin (TH)	1	B565_0938

3.14 Analysis of Antibiotic Resistance

To further investigate the drug-resistant characteristics of strain SJ4, the main drug-resistant genes of SJ4 were predicted (Table 4). The results showed that the SJ4 genome contains drug-resistant genes related to tetracyclines, fluoroquinolones, aminoglycosides, macrolides, chloramphenicol, and cephalosporins (Fig. 11). These genes mainly confer resistance to antibiotics through mechanisms such

as antibiotic target alteration, antibiotic target replacement, reduced permeability to antibiotics, antibiotic inactivation, and antibiotic efflux.

Table 4
Physiological and biochemical characteristics of strain SJ4.

Antibiotics	Number	genes
tetracycline antibiotic	7	<i>tet(35) H-NS adeB TolC acrA acrB</i>
fluoroquinolone antibiotic	8	<i>H-NS CRP TolC rsmA mdhH acrA acrB</i>
aminoglycoside antibiotic	1	<i>TolC</i>
aminocoumarin antibiotic	1	<i>TolC</i>
streptomycin antibiotic	1	<i>vatF</i>
cephalosporin	8	<i>H-NS OmpA TolC OXA-12 golS acrA acrB</i>
macrolide antibiotic	4	<i>H-NS CRP TolC</i>
penicillane	9	<i>H-NS CRP OmpA TolC OXA-12 golS acrA acrB</i>
rifamycin antibiotic	6	<i>rphB TolC rpoB2 acrA acrB</i>
glycylcycline	4	<i>adeB TolC acrA acrB</i>
diaminopyrimidine antibiotic	2	<i>dfrA3 rsmA</i>
carbapenem	4	<i>cphA3 OmpA TolC golS</i>
monobactam	2	<i>OmpA golS</i>
penem	3	<i>OmpA TolC golS</i>
cephamycin	5	<i>H-NS OmpA TolC golS</i>
peptide antibiotic	6	<i>TolC bacA YojI rpoB2 MCR-7.1</i>
chloram phenicols	6	<i>TolC catB9 golS rsmA acrA acrB</i>
triclosan	3	<i>TolC acrA acrB</i>
Nitroimidazole antibiotic	1	<i>msbA</i>

4. Discussion

As a common opportunistic pathogen in freshwater fish in China, *A. veronii* has been recognized as one of the major pathogens in the aquaculture industry (Ran et al. 2018). Recently, it is rapidly increased of the cases of economic fish death, exhibiting pathological signs such as ulceration, organ hemorrhage and severe ascites, as well as abdominal enlargement and redness (Zhu et al. 2022). Previous studies show that *A. veronii* has been confirmed to be the pathogen of ulcerative disease. Wang et al. (2021)

reported that the *A. veronii* strain 18BJ181 which was firstly isolated from diseased *L. maculatus*, caused acute death in aquaculture. Mohamed *et al.* (2017) reported the *A. veronii* to be the most predominant pathogen of *O. niloticus*. In this study, *A. veronii* SJ4 was isolated from diseased *S. chuatsi*, and the major pathological symptoms exhibit gill pallor, muscle bleeding and necrosis, fin erosion, as well as abdominal enlargement, redness and swelling. Experimental infection in vivo showed that the LD₅₀ of *A. veronii* SJ4 to *S. chuatsi* was 3.8×10^5 CFU/mL and the *S. chuatsi* infected by *A. veronii* developed similar clinical signs to the naturally infected fish, suggesting that the isolate SJ4 has the high virulence to *S. chuatsi*.

It is well known of *Aeromonas* spp. to possess several virulence factors, such as adhesion factor, flagellum, exotoxins, endotoxins, and extracellular enzymes, *etc* (Castro *et al.* 2003). Previous studies have demonstrated the crucial role of extracellular products (ECPs) in the pathogenic-mechanism of bacteria pathogens (Sharma *et al.* 2017). ECPs produced by *Aeromonas* genus bacteria, including *A. veronii* and *A. hydrophila*, have been proved to cause huge damage to organisms (Gonz *et al.* 2002). The haemolysin and aerolysin proteins promote the process of pathogen invasion in host, while lipases catalyze the hydrolysis of membrane lipids, leading to intestinal damage (Sughra *et al.* 2022). Through these virulence factors, the bacteria pathogen adheres to the surface of host tissue cells, disrupts the immune system, and hence starts colonization. In this study, it was observed that *A. veronii* SJ4 exhibited a dense coverage of long fimbriae upon microscopic observation. This finding implies that *A. veronii* SJ4 may possess a high level of both adhesion and virulence. *A. veronii* SJ4 has demonstrated various enzymatic activities such as caseinase, Dnase, gelatinase, and hemolysin, which may facilitate the bacterium's ability of invading the host. Moreover, the presence of virulence genes including *act*, *fim*, *flgM*, *ompA*, *lip*, *hly*, *aer*, and *eprCAL* plays a crucial role in protein code and toxin secretion, which contribute to the pathogenicity of *A. veronii* SJ4. The various toxins and enzymes expressed by these genes have the potential to inflict damage on host cells, leading to their deterioration.

Whole genome sequencing technology plays a critical role in molecular epidemiology research of pathogenic bacteria, as it reveals the genomic characteristics, infers transmission routes and epidemiological features, and aids in infection control and prevention (De *et al.* 2019). Zhou *et al.* (2022) used whole-genome sequencing to reveal the virulence and resistance mechanisms of non-O1 *Vibrio cholerae*, the pathogen of shrimp disease. Pang *et al.* (2015) conducted whole-genome sequencing analysis of *A. hydrophila*, identifying three metabolic pathways unique to the epidemic strain. Kang *et al.* (2016) sequenced the whole genome of the highly virulent *A. veronii* strain TH0426 and also determined the genome framework of the weakly virulent strain AV161 and the non-pathogenic strain CL8155, revealing the differences among *A. veronii* strains with strong, weak and no virulence at the genome level through comparative analysis. In present study, the complete genome nucleotide sequence of *A. veronii* SJ4 was determined with a total of 4079 predicted genes, among a GC content of 58.95% and 124 tRNA genes, 43 sRNA genes, and 31 rRNA genes. A considerable quantity of genes were identified and annotated within the NR, COG/KOG, GO, Swissprot, eggNOG, KEGG, Pfam pathways. Notably, these pathways have been previously linked to various human diseases. Additionally, earlier investigations have demonstrated that *A. veronii* can induce numerous maladies, including toxemia, diarrhea, and

endocarditis, among others. This evidence underscores the potential risk that *A. veronii* strain SJ4 may pose to human health (Liu et al. 2022).

The pathogenesis of *Aeromonas* infection is a complex process involving multiple factors. The initial stages of bacterial pathogenicity entail movement, invasiveness and colonization. Specifically, the single polar flagellum allows the *Aeromonas* genus bacteria to swim in liquid environments, and the extra lateral flagellar system contributed to the collective motions and biofilm formation of 60% *Aeromonas* genus bacteria (Fern and Figueras 2020). In the present study, a total of about 128 genes encoding for flagellar component protein were determined in the *A. veronii* SJ4 genome. Besides several flagellar related genes, many virulence related gene encoding for extracellular toxins and enzymes have a potential virulence property to the *Aeromonas* genus. The genes encoding for caseinase, dnase, gelatinase, and hemolysin were also determined in *A. veronii* SJ4 genome, which is consistent with the phenotypic results of extracellular enzyme activity. Hemolysin and aerolysin play a critical role in host tissue damage, bacterial invasiveness and colonization, as well as the suppression of immune system, which contribute to the phenotypic symptom of hemorrhagic septicemia. Additionally, the presence rate of hemolysin, aerolysin, lipases, and serine proteinase is remarkably high among *Aeromonas* isolates derived from diseased fish (Tyagi et al. 2022). *A. veronii* SJ4 genome also carried 15, 15, 6, 5, 7 genes involved in T2SS T3SS T4SS T6SS T7SS biosynthesis, respectively. Bacteria use T2SS to release cytoplasmic proteins, including virulence factors like hemolysin, aerolysin, caseinase and dnase in *Aeromonas* (Matys et al. 2020). The bacterial effector proteins could directly invade into the host cell with a needle-like structure created by T3SS, which disrupt signaling pathways and cytoskeleton, as well as induce apoptosis (Zeb et al. 2019). T4SS transports DNA, proteins, and other molecules through multiple proteins, while T6SS indirectly interacts with host cells through peptidoglycan-like effectors, such as *Vibrio*'s T6SS uses toxic effectors with an actin cross-linking domain to directly act on eukaryotic cells (Wang et al. 2016).

Multiple antibiotic resistance genes related to antibiotic target alteration, antibiotic target replacement, reduced permeability to antibiotics, antibiotic inactivation and antibiotic efflux, were also determined in the *A. veronii* SJ4 genome. However, it is extremely complicated of resistance mechanisms in pathogenic bacteria that the bacteria could control the antibiotic content in the cells through complex biochemical pathways, or change/degrade the antibiotics through enzymatic action. Moreover, the bacteria gene mutation may also infect the effectiveness of the antibiotics (Munita *et al.* 2016). Thus, it is not inevitably that antibiotic resistance genes could be transformed into antibiotic resistance phenotype. In the present study, despite that many antibiotic-related genes (fluoroquinolone, penicillin tetracycline, *etc.*) were determined in the genome of *A. veronii* SJ4, it was observed that no resistance against some tested antibiotics (florfenicol, ofloxacin, enrofloxacin, *etc.*) in antibiotics susceptibility testing (the supplementary table 1). The observed phenomenon may be attributed to either the non-functionality of the efflux pump in *A. veronii* SJ4, the absence of antibiotic gene expression, or the dysfunction of the enzyme itself (Mart and Baquero 2002).

5. Conclusion

In summary, the *A. veronii* SJ4 was identified as a high virulence pathogen to *S. chuatsi* in this study. After whole genome sequencing, many virulence-related genes and antibiotic resistance genes are annotated in the database. The present study provides theoretical basis to clarify characteristics, pathogenicity, antibiotic resistance and virulence factors of highly pathogenic *A. veronii* at the molecular level.

Declarations

Author Contributions Xinhai Zhu: writing—original draft, methodology, conceptualization, data curation. Lijie Qin: methodology, data curation. Qieqi Qian: methodology, data curation. Yujie Zhu: methodology, data curation. Xiaojian Gao: writing—review. Qun Jiang: methodology. Jun Wang: data curation. Guoxing Liu: funding acquisition. Xiaojun Zhang: writing—review, conceptualization, funding acquisition.

Dunding This work was supported by the “JBGS” Project of Seed Industry Revitalization in Jiangsu Province (JBGS [2021] 132).

Data Availability The datasets generated during and/or analyzed during the current study are available from the corresponding author on reasonable request.

Ethics statement All treatments involving animals were carried out under the strict guidelines of Animal Experiment Ethics Committee of Yangzhou University.

Conflicts of Interest The authors declare no conflict of interest.

References

1. Behrens A, Karber L (1953) Determination of LD50. Screening in Pharmacology. New York, NY: Academic Press.
2. Brenner D J, Krieg N R, Staley J T (2021) Bergey’s Manual of Systematic Bacteriology 2nd edn, vol 2, part B, Springer USA 404–406.
3. Changfu C, Weizhou S, Guizhen Z, Mingzhen L (1995) Isolation and identification of pathogenic bacteria causing roted gill disease in mandarin fish *Siniperca chuatsi* Basilewsky. Hua Zhong Nong ye da xue xue bao = Journal Huazhong (Central China) Agricultural University 14(3): 263–266.
4. Castro-Escarpulli G, Figueras M J, Aguilera-Arreola G, Soler L, Fernández-Rendón E, Aparicio G O, Guarro J, Chacon M R (2003) Characterisation of *Aeromonas* spp. isolated from frozen fish intended for human consumption in Mexico. Int J Food Microbiol 84(1): 41–49.
5. Chen N, Jiang J, Gao X J, Li X X, Zhang Y, Liu X D, Yang H, Bing X W, Zhang X J (2018) Histopathological analysis and the immune related gene expression profiles of mandarin fish (*Siniperca chuatsi*) infected with *Aeromonas hydrophila*. Fish Shellfish Immun 83: 410–41785.
6. Donkor E S (2013) Sequencing of bacterial genomes: principles and insights into pathogenesis and development of antibiotics. Genes 4(4): 556–572.

7. Dong H T, Techatanakitarnan C, Jindakittikul P, Thaiprayoon A, Taengphu S, Charoensapsri W, Khunrae P, Rattanaojpong T, Senapin S (2017) *Aeromonas jandaei* and *Aeromonas veronii* caused disease and mortality in Nile tilapia, *Oreochromis niloticus* (L.). J Fish Dis 40(10): 1395–1403.
8. De Maio N, Shaw L P, Hubbard A, George S, Sanderson N D, Swann J, Wick R, AbuOun M, Stubberfield E, Hoosdally S J, Crook D W, Peto T E A, Sheppard A E, Bailey M J, Read D S, Anjum M F, Walker S, Stoesser N (2019) Comparison of long-read sequencing technologies in the hybrid assembly of complex bacterial genomes. Microbiol Genomics 5(9): e000294.
9. Fernández-Bravo A, Figueras M J (2020) An update on the genus *Aeromonas*: Taxonomy, epidemiology, and pathogenicity. Microorganisms 8(1): 129.
10. González-Serrano C J, Santos J A, García-López M L, Otero A (2002) Virulence markers in *Aeromonas hydrophila* and *Aeromonas veronii* biovar *sobria* isolates from freshwater fish and from a diarrhoea case. J Appl Microbiol 93(3): 414–419.
11. Gao X, Tong S, Zhang S, Chen Q, Jiang Z, Jiang Q, Wei W, Zhu J, Zhang X (2020) *Aeromonas veronii* associated with red gill disease and its induced immune response in *Macrobrachium nipponense*. Aquac Res 51(12): 5163–5174.
12. Haslinger-Löffler B, Kahl B C, Grundmeier M, Strangfeld K, Wagner B, Fischer U, Cheung A L, Peters G, Schulze OK, Sinha B (2005) Multiple virulence factors are required for *Staphylococcus aureus*-induced apoptosis in endothelial cells. Cell Microbiol 7(8): 1087–1097.
13. Huang X, Wu C, Deng Y, Wang K, Geng Y, Zhao J (2010) Pathohistological observation of *Ictalurus punctatus* infected with *Aeromonas veronii*. Chinese Veterinary Science/Zhongguo Shouyi Kexue 40(7): 738–742.
14. Hassan M A, Noureldin E A, Mahmoud M A, Fita N A (2017) Molecular identification and epizootiology of *Aeromonas veronii* infection among farmed *Oreochromis niloticus* in Eastern Province, KSA. The Egyptian Journal of Aquatic Research 43(2): 161–167.
15. Janda J M, Abbott S L (2010) The genus *Aeromonas*: taxonomy, pathogenicity, and infection. Clin Microbiol Rev 23(1): 35–73.
16. Kim J D, Do J W, Choi H S, Seo J S, Jung S H, Jo H I, Park M A, Lee N S, Park S W (2013) Pathological changes in cultured Korean catfish (*Silurus asotus*) artificially infected with *Aeromonas veronii*. Korean Journal of Environmental Biology 31(4): 486–492.
17. Kang Y, Pan X, Xu Y, Siddiqui S A, Wang C, Shan X, Qian A (2016) Complete genome sequence of the fish pathogen *Aeromonas veronii* TH0426 with potential application in biosynthesis of pullulanase and chitinase. J Biotechnol 227: 81–82.
18. Kumar S, Stecher G, Tamura K (2016) MEGA7: molecular evolutionary genetics analysis version 7.0 for bigger datasets. Mol Biol Evol 33(7): 1870–1874.
19. Kaur A, Holeyappa S A, Bansal N, Kaur V I, Tyagi A (2020) Ameliorative effect of turmeric supplementation in feed of *Labeo rohita* (Linn.) challenged with pathogenic *Aeromonas veronii*. Aquacult Int 28: 1169–1182.

20. Luo X, Fu X, Liao G, Chang O, Huang Z, Li N (2017) Isolation, pathogenicity and characterization of a novel bacterial pathogen *Streptococcus uberis* from diseased mandarin fish *Siniperca chuatsi*. *Microb Pathogenesis* 107: 380–389.
21. Lin Q, Li J, Fu X, Liu L, Liang H, Niu Y, Huang C, Huang Z, Mo Z, Li N (2020) Hemorrhagic gill disease of Chinese perch caused by *Aeromonas salmonicida* subsp. *salmonicida* in China. *Aquaculture* 519: 734775.
22. Liu F, Yuwono C, Tay A C Y, Wehrhahn M C, Riordan S M, Zhang L (2022) Analysis of global *Aeromonas veronii* genomes provides novel information on source of infection and virulence in human gastrointestinal diseases. *BMC genomics* 23(1): 1–15.
23. Liu G, Li J, Jiang Z, Zhu X, Gao X, Jiang Q, Wang J, Wei W, Zhang X (2022) Pathogenicity of *Aeromonas veronii* causing mass mortalities of *Odontobutis potamophila* and its induced host immune response. *Fish Shellfish Immun* 125: 180–189.
24. Martínez J L, Baquero F (2002) Interactions among strategies associated with bacterial infection: pathogenicity, epidemicity, and antibiotic resistance. *Clin Microbiol Rev* 15(4): 647–679.
25. Miller W R, Munita J M, Arias C A (2014) Mechanisms of antibiotic resistance in enterococci. *Expert Rev Anti-Infe* 12(10): 1221–1236.
26. Mishra S S, Rakesh D, Dhiman M, Choudhary P, Debbarma J, Sahoo S N, Mishra C K (2017) Present status of fish disease management in freshwater aquaculture in India: state-of-the-art-review. *Journal of Aquaculture & Fisheries* 1(003): 14.
27. Matys J, Turska-Szewczuk A, Sroka-Bartnicka A (2020) Role of bacterial secretion systems and effector proteins—insights into *Aeromonas* pathogenicity mechanisms. *Acta Biochim Pol* 67(3): 283–293.
28. Nailis H, Kucharíková S, Řičicová M, Van Dijck P, Deforce D, Nelis H, Coenye T (2010) Real-time PCR expression profiling of genes encoding potential virulence factors in *Candida albicans* biofilms: identification of model-dependent and-independent gene expression. *BMC microbiol* 10(1): 1–11.
29. Pang M, Jiang J, Xie X, Wu Y, Dong Y, Kwok A H, Zhang W, Yao H, Lu C, Leung F C, Liu Y (2015) Novel insights into the pathogenicity of epidemic *Aeromonas hydrophila* ST251 clones from comparative genomics. *Sci Rep-UK* 5(1): 9833.
30. Ran C, Qin C, Xie M, Zhang J, Li J, Xie Y, Wang Y, Li S, Liu L, Fu X, Lin Q, Li N, Liles M R, Zhou Z (2018) *Aeromonas veronii* and *aerolysin* are important for the pathogenesis of motile aeromonad septicemia in cyprinid fish. *Environ Microbiol* 20(9): 3442–3456.
31. Sreedharan K, Philip R, Singh I B (2011) Isolation and characterization of virulent *Aeromonas veronii* from ascitic fluid of oscar *Astronotus ocellatus* showing signs of infectious dropsy. *Dis Aquat Organ* 94(1): 29–39.
32. Sharma A K, Dhasmana N, Dubey N, Kumar N, Gangwal A, Gupta M, Singh Y (2017) Bacterial virulence factors: secreted for survival. *Indian J Microbiol* 57: 1–10.
33. Smyrli M, Prapas A, Rigos G, Kokkari C, Pavlidis M, Katharios P (2017) *Aeromonas veronii* infection associated with high morbidity and mortality in farmed European seabass *Dicentrarchus labrax* in

- the Aegean Sea, Greece. *Fish Pathol* 52(2): 68–81.
34. Shameena S S, Kumar K, Kumar S, Kumar S, Rathore G (2020) Virulence characteristics of *Aeromonas veronii* biovars isolated from infected freshwater goldfish (*Carassius auratus*). *Aquaculture* 518: 734819.
 35. Shen Y, Wu Y, Wang Y, Li L, Li C, Zhao Y, Yang S (2021) Contribution of autochthonous microbiota succession to flavor formation during Chinese fermented mandarin fish (*Siniperca chuatsi*). *Food Chem* 348: 129107.
 36. Sughra F, Hafeez-ur-Rehman M, Abbas F, Altaf I, Hassan Z, Bhatti A, Ali K (2022) Molecular characterisation and genetic analysis of aerolysin and haemolysin in *Aeromonas hydrophila* isolated from diseased *Labeo rohita* by polymerase chain reaction. *J Fish* 10(3): 103402–103402.
 37. Tekedar H C, Kumru S, Blom J, Perkins A D, Griffin M J, Abdelhamed H, Karsi A, Lawrence M L (2019) Comparative genomics of *Aeromonas veronii*: Identification of a pathotype impacting aquaculture globally. *PloS one* 14(8): e0221018.
 38. Tyagi A, Sharma C, Srivastava A, Kumar B N, Pathak D, Rai S (2022) Isolation, characterization and complete genome sequencing of fish pathogenic *Aeromonas veronii* from diseased *Labeo rohita*. *Aquaculture* 553: 738085.
 39. Wang P, Wen Z, Li B, Zeng Z, Wang X (2016) Complete genome sequence of *Vibrio alginolyticus* ATCC 33787T isolated from seawater with three native megaplasms. *Mar Genom* 28: 45–47.
 40. Wang B, Mao C, Feng J, Li Y, Hu J, Jiang B, Gu Q, Su Y (2021) A first report of *Aeromonas veronii* infection of the sea bass, *Lateolabrax maculatus* in China. *Front Vet Sci* 7: 600587.
 41. Zhang X J, Bai X S, Yan B L, Bi K R, Qin L (2014) *Vibrio harveyi* as a causative agent of mass mortalities of megalopa in the seed production of swimming crab *Portunus trituberculatus*. *Aquacult Int* 22: 661–672.
 42. Zhou W, Zhang Y, Wen Y, Ji W, Zhou Y, Ji Y, Liu X, Wang W, Asim M, Liang X, Ai T, Lin L (2015) Analysis of the transcriptomic profilings of Mandarin fish (*Siniperca chuatsi*) infected with *Flavobacterium columnare* with an emphasis on immune responses. *Fish Shellfish Immun* 43(1): 111–119.
 43. Zeb S, Shah M A, Yasir M, Awan H M, Prommeenate P, Klanchui A, Wren B W, Thomson N, Bokhari H (2019) Type III secretion system confers enhanced virulence in clinical non-O1/non-O139 *Vibrio cholerae*. *Microb Pathogenesis* 135: 103645.
 44. Zhang H P, Chen M Y, Xu Y X, Xu G Y, Chen J R, Wang Y M, Kang Y H, Shan X F, Kong L C, Ma H X (2020) An effective live attenuated vaccine against *Aeromonas veronii* infection in the loach (*Misgurnus anguillicaudatus*). *Fish Shellfish Immun* 104: 269–278.
 45. Zhou Y, Gu S, Li J, Ji P, Zhang Y, Wu C, Jiang Q, Gao X, Zhang X (2022) Complete genome analysis of highly pathogenic non-O1/O139 *Vibrio cholerae* isolated from *Macrobrachium rosenbergii* reveals pathogenicity and antibiotic resistance-related genes. *Front Vet Sci* 9: 882–885.
 46. Zhu X, Qian Q, Wu C, Zhu Y, Gao X, Jiang Q, Wang J, Liu G, Zhang X (2022) Pathogenicity of *Aeromonas veronii* Causing Mass Mortality of Largemouth Bass (*Micropterus salmoides*) and Its

Supplementary Table

Supplementary Table 1 is not included with this version

Figures

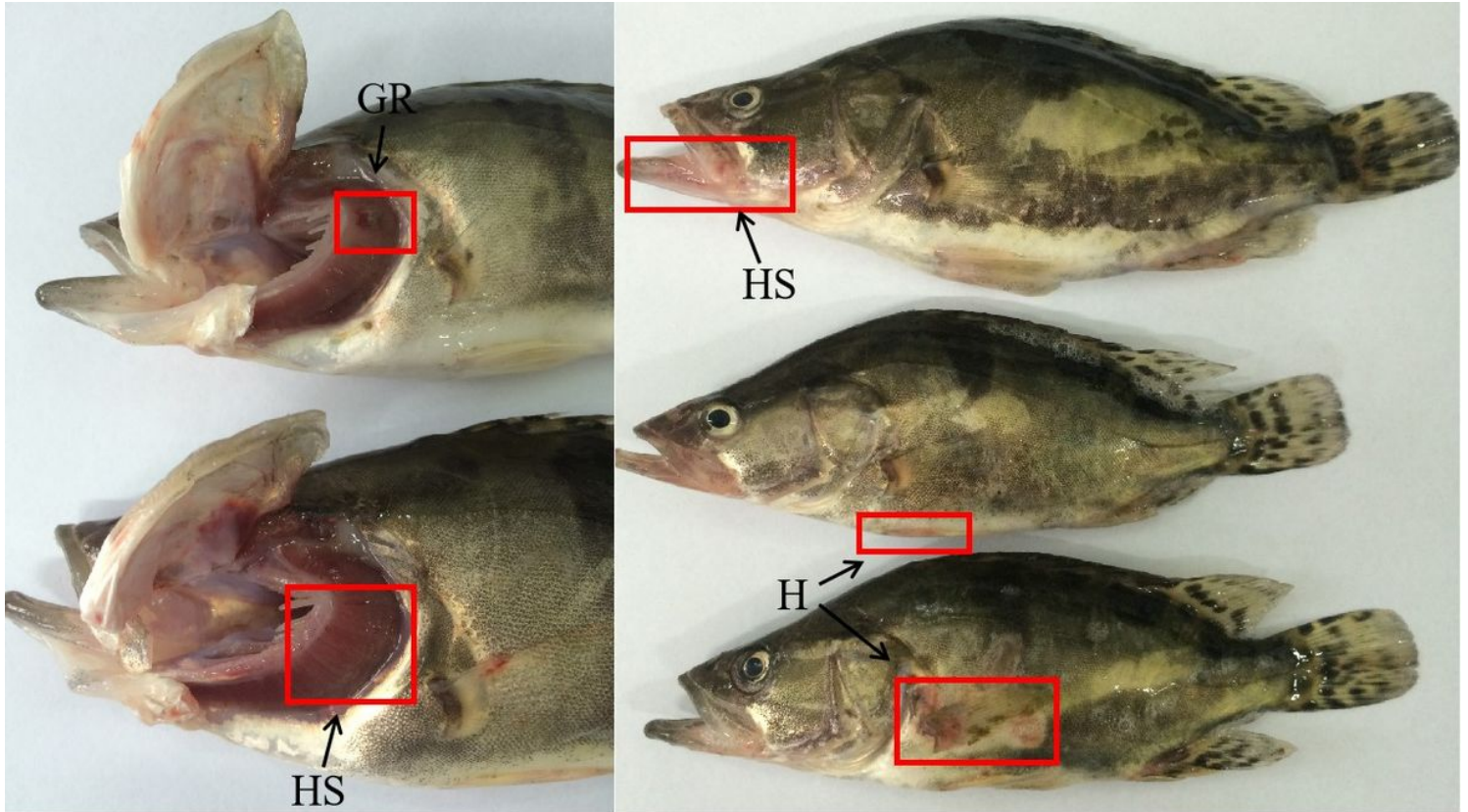


Figure 1

External clinical symptoms of experimentally infected *S. chuatsi*. GR - gill rot; HS – hemorrhage spot; H - hemorrhage.

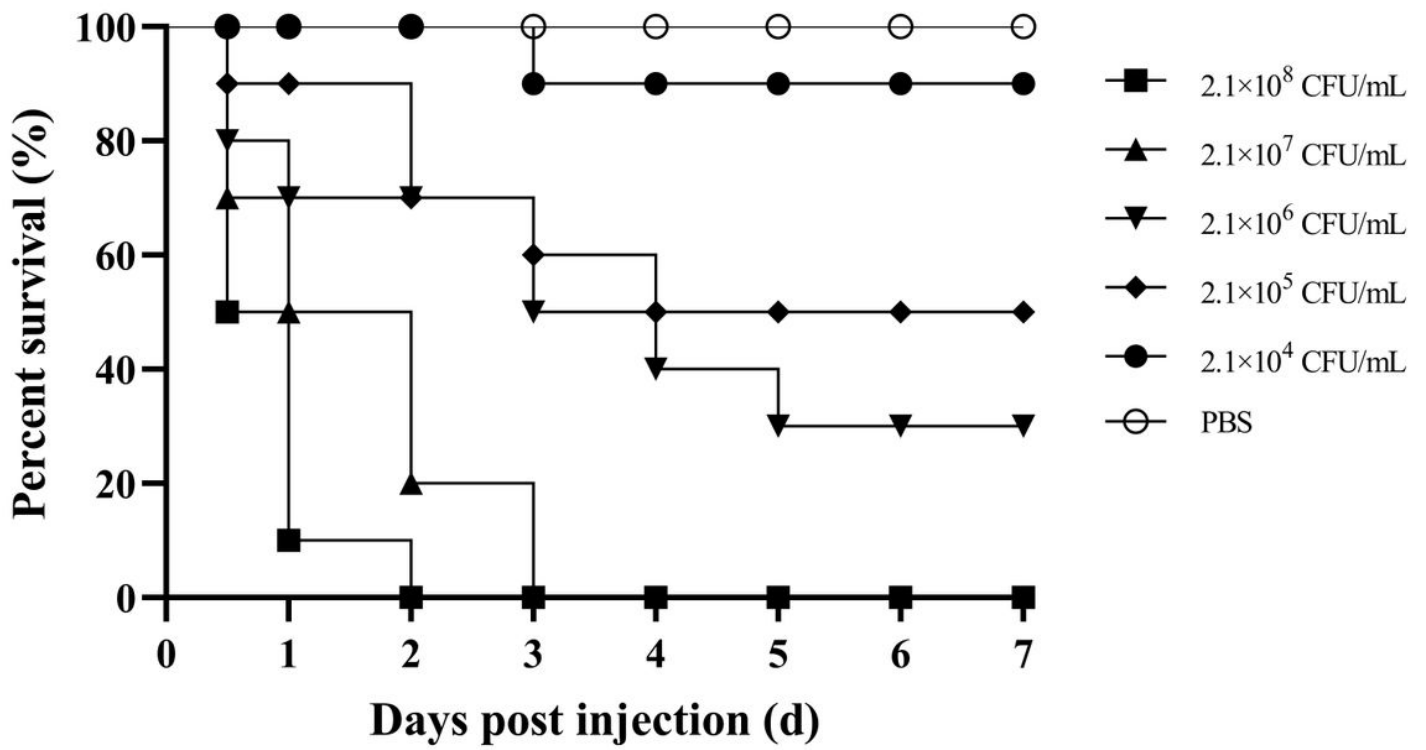


Figure 2

The survival rates of largemouth bass challenged by SJ4.

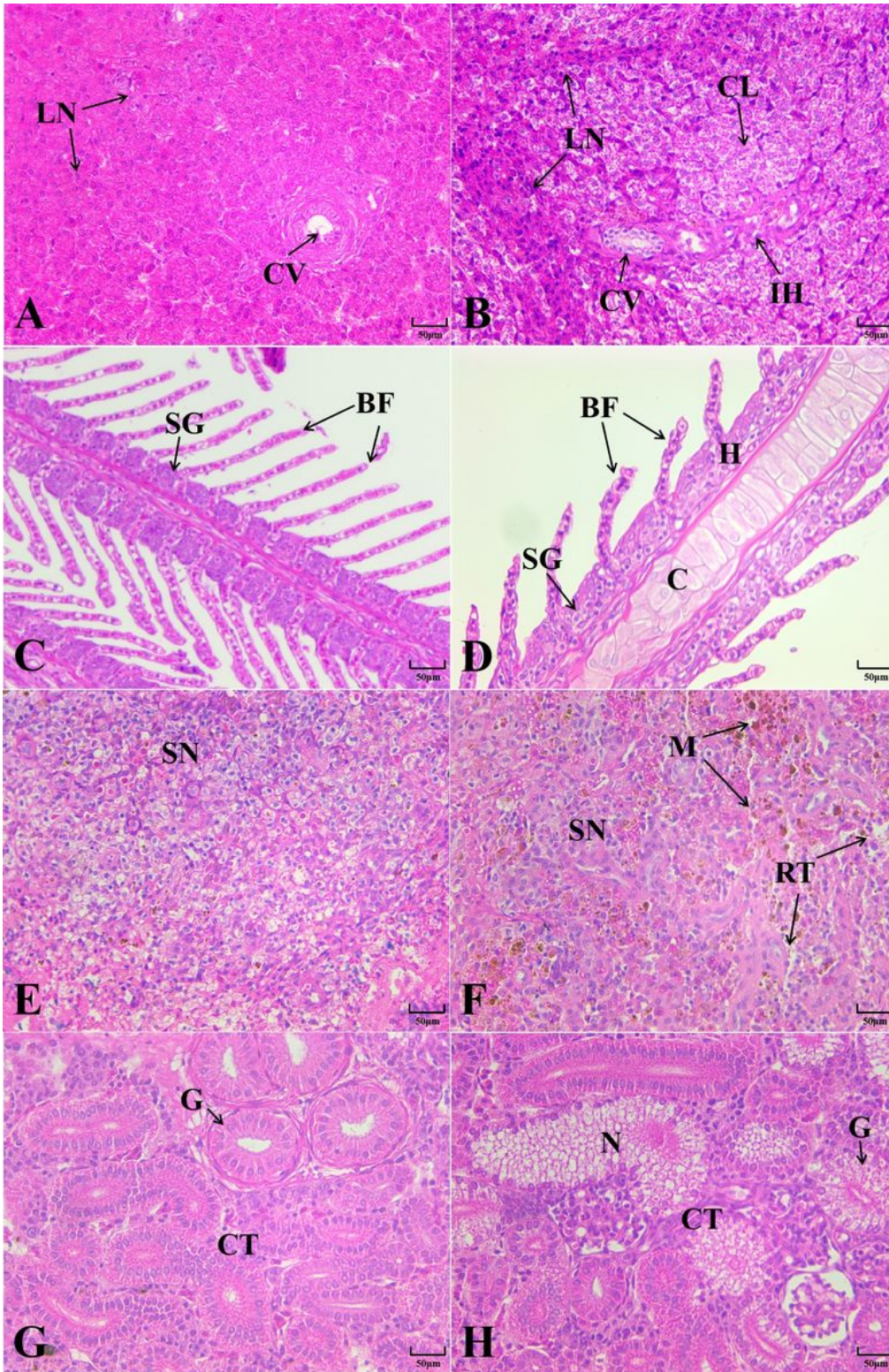


Figure 3

Histological changes of *S. chuatsi* infected by the isolate SJ4. CV represents Swollen Central Vein; LN represents liver nucleus; CL represents cytoplasmic lysis; IH represents interstitial hyperplasia; BF represents branchial filament; SG represents the secondary gill lamellae; H represents Hypertrophy; C represents Chondrocyte; SN represents spleen nucleus; M represents macrophage; RT represents rupture; G represents glomerulus; CT represents connective tissue; N represents necrosis.



30.tif
10:02:42 a 05-05-17
TEM Mode: Imaging

500 nm
HV=80.0kV
Direct Mag: 6000x
AMT Camera System

Figure 4

Electron micrograph of GJL1, bar = 0.5 μm .

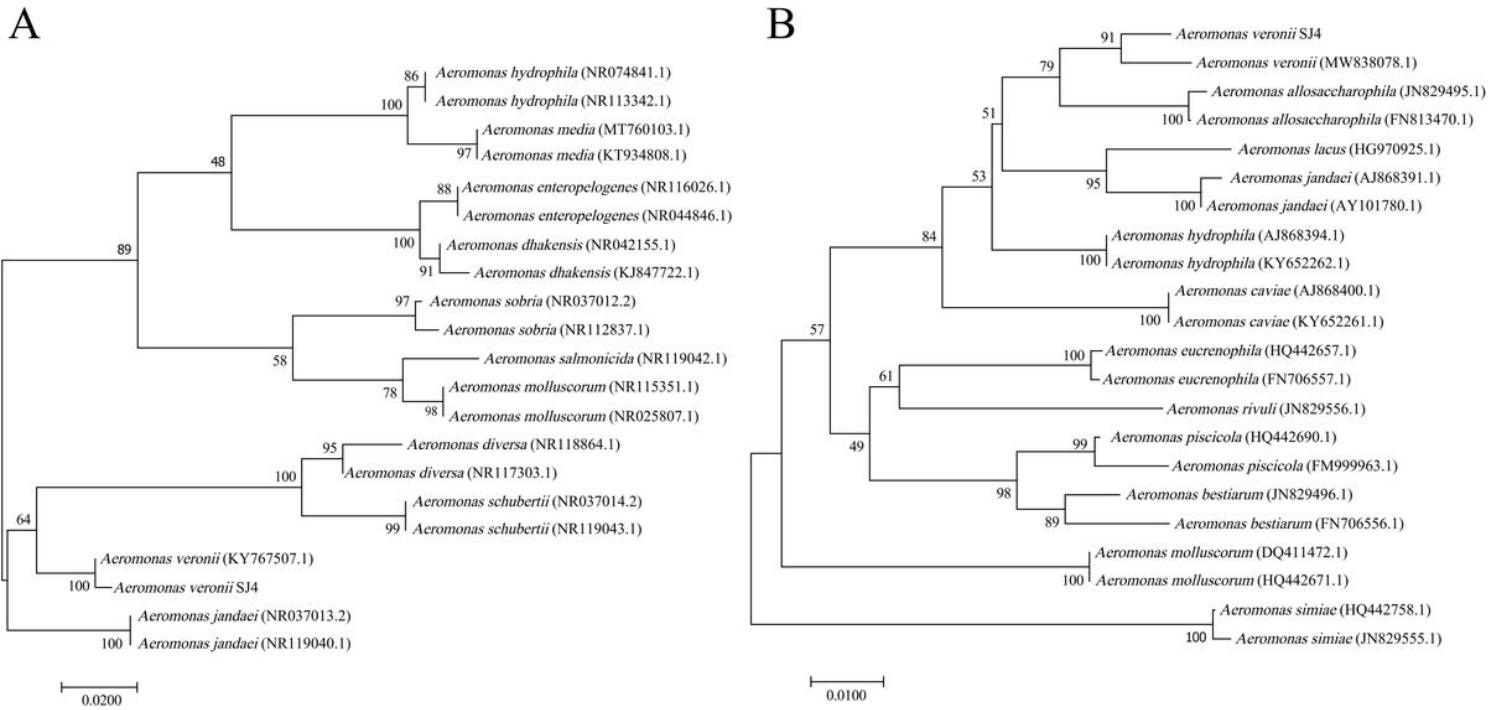


Figure 5

(A) Phylogenetic tree of *Aeromonas* species based on 16S rRNA sequences. (B) Phylogenetic tree of *Aeromonas* species based on *gyrB* sequences.

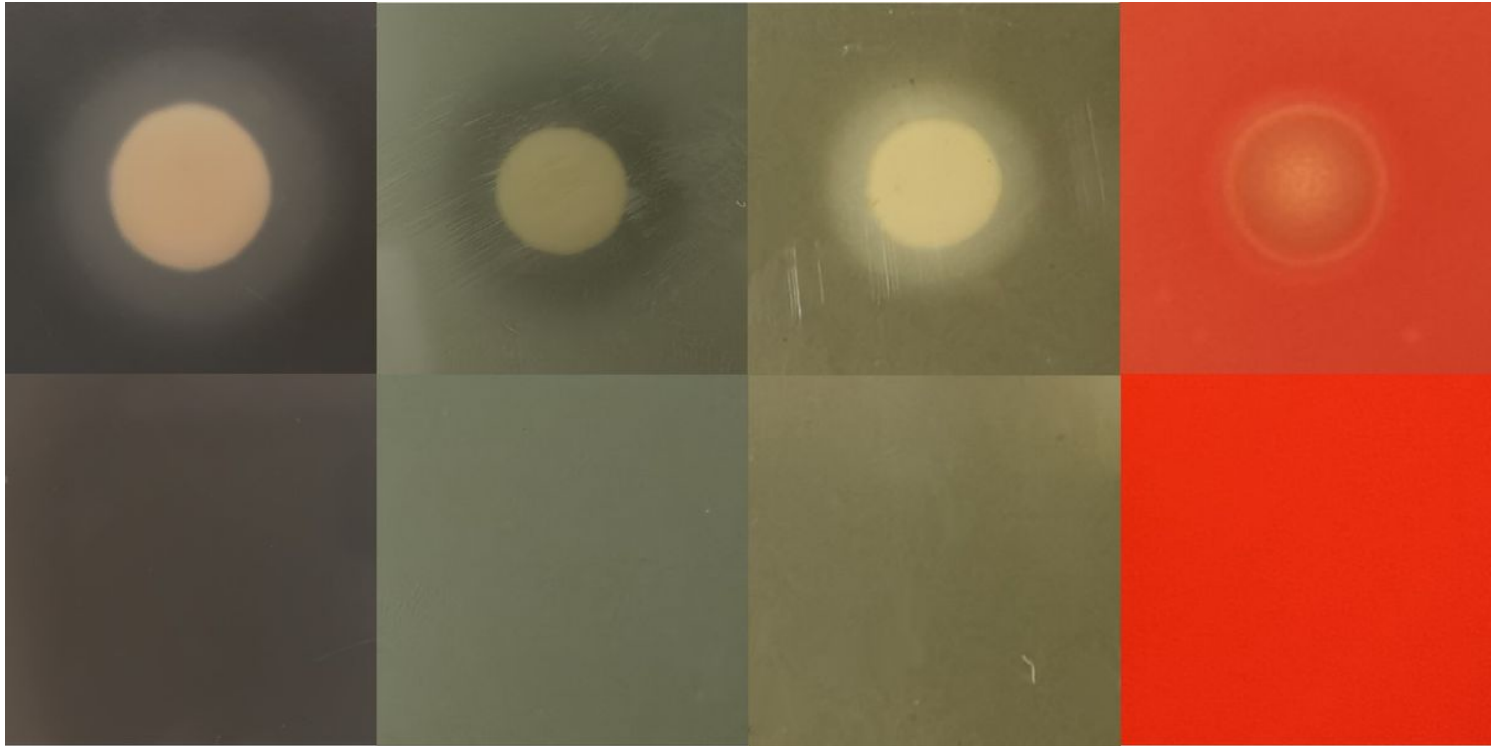
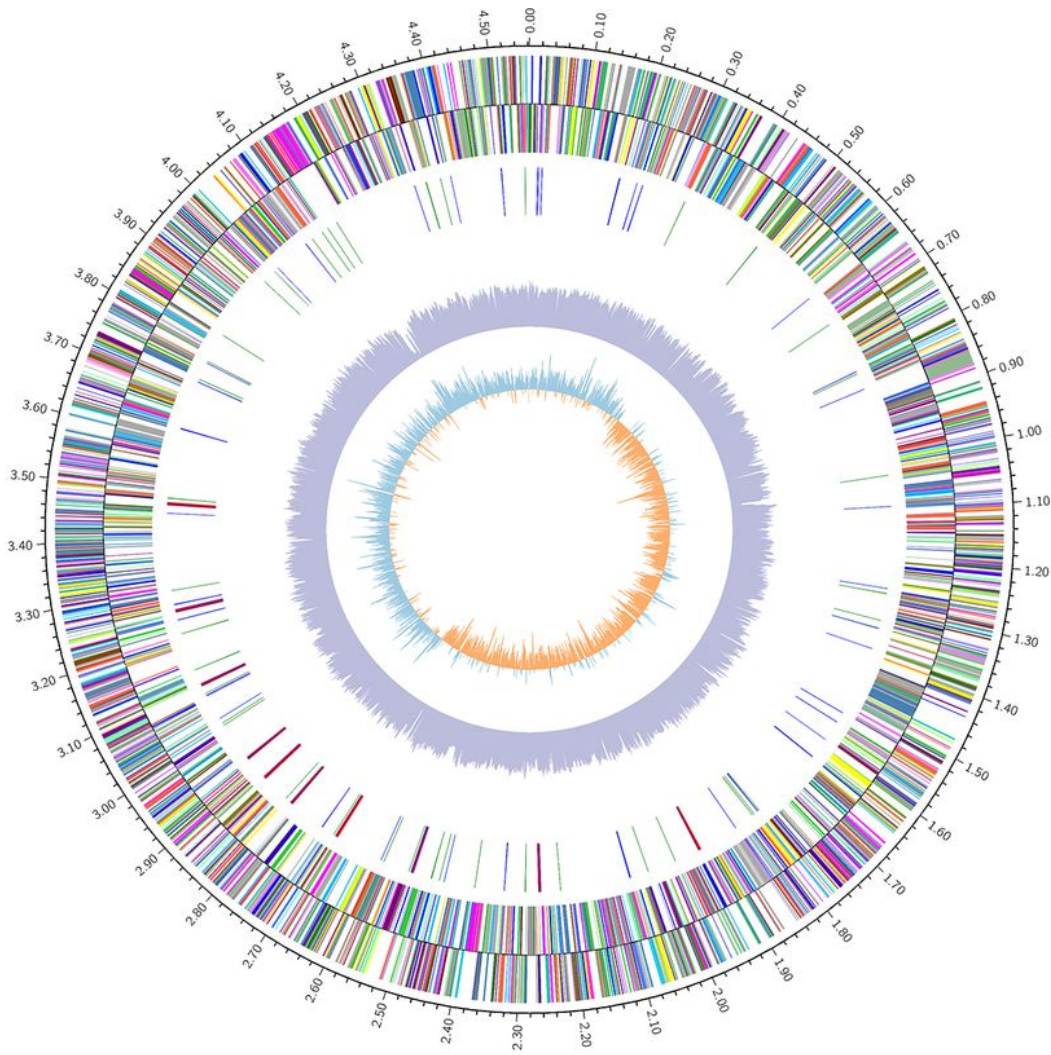


Figure 6

The extracellular enzyme test results of *A. veronii* SJ4.



- | | |
|--|---|
| ■ A: RNA processing and modification | ■ N: Cell motility |
| ■ B: Chromatin structure and dynamics | ■ O: Posttranslational modification, protein turnover, chaperones |
| ■ C: Energy production and conversion | ■ P: Inorganic ion transport and metabolism |
| ■ D: Cell cycle control, cell division, chromosome partitioning | ■ Q: Secondary metabolites biosynthesis, transport and catabolism |
| ■ E: Amino acid transport and metabolism | ■ R: General function prediction only |
| ■ F: Nucleotide transport and metabolism | ■ S: Function unknown |
| ■ G: Carbohydrate transport and metabolism | ■ T: Signal transduction mechanisms |
| ■ H: Coenzyme transport and metabolism | ■ U: Intracellular trafficking, secretion, and vesicular transport |
| ■ I: Lipid transport and metabolism | ■ V: Defense mechanisms |
| ■ J: Translation, ribosomal structure and biogenesis | ■ W: Extracellular structures |
| ■ K: Transcription | ■ Y: Nuclear structure |
| ■ L: Replication, recombination and repair | ■ Z: Cytoskeleton |
| ■ M: Cell wall/membrane/envelope biogenesis | ■ No assigned COG |

Figure 7

Circular genome map of *A. veronii* SJ4.

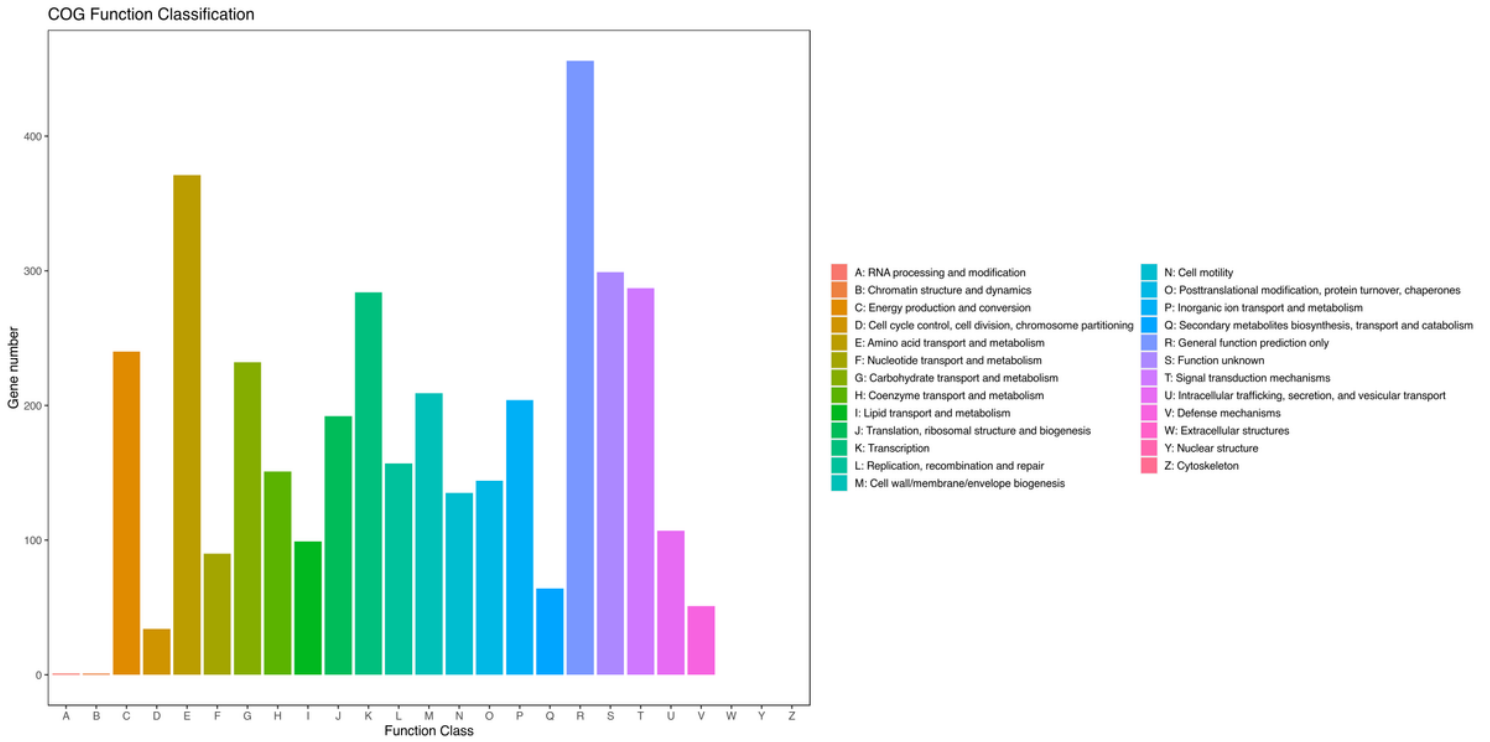


Figure 8

The Clusters of Orthologous Genes (COG) functional annotation in the whole genome of *A. veronii* SJ4.

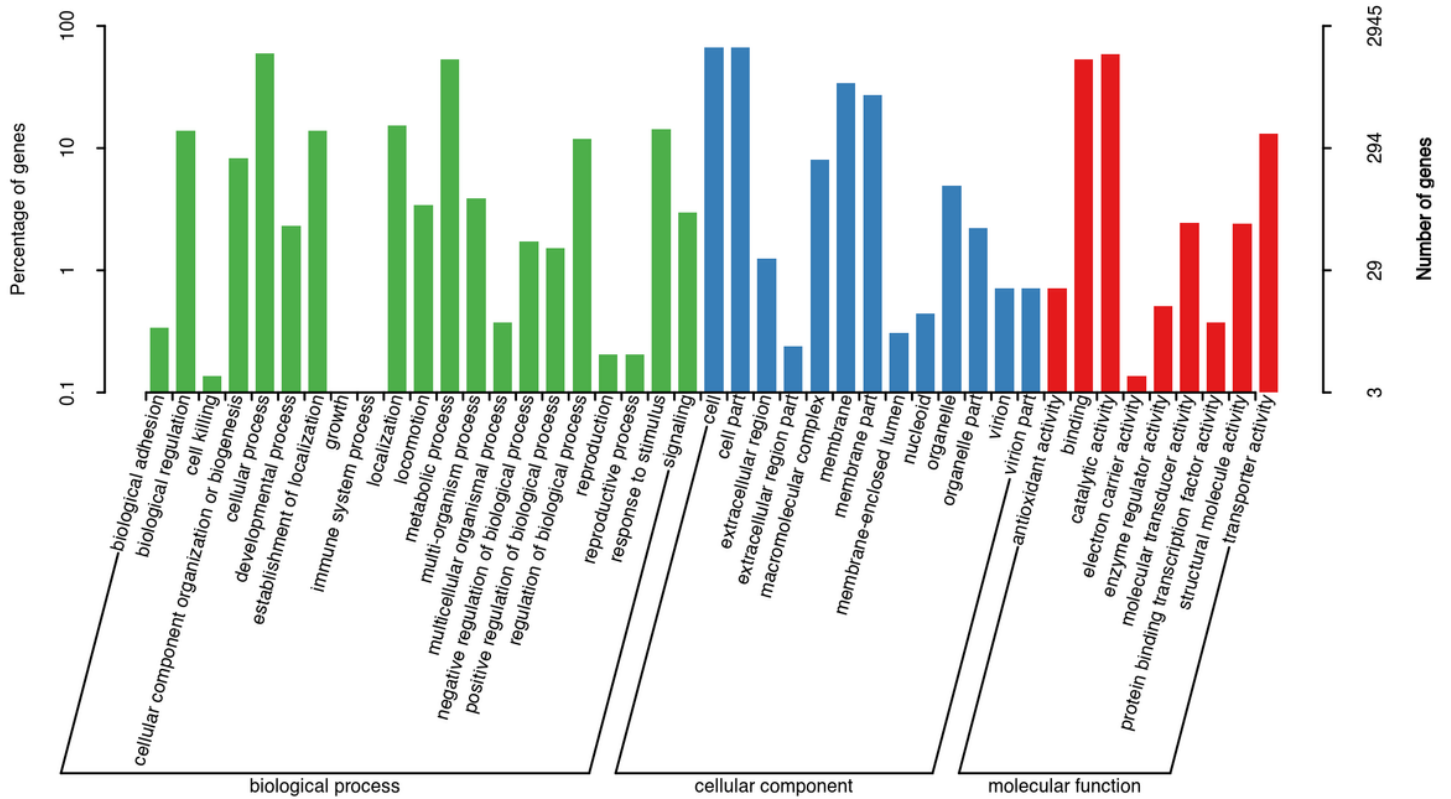


Figure 9

Gene Oncology (GO) functional annotation in the whole genome of *A. veronii* SJ4.

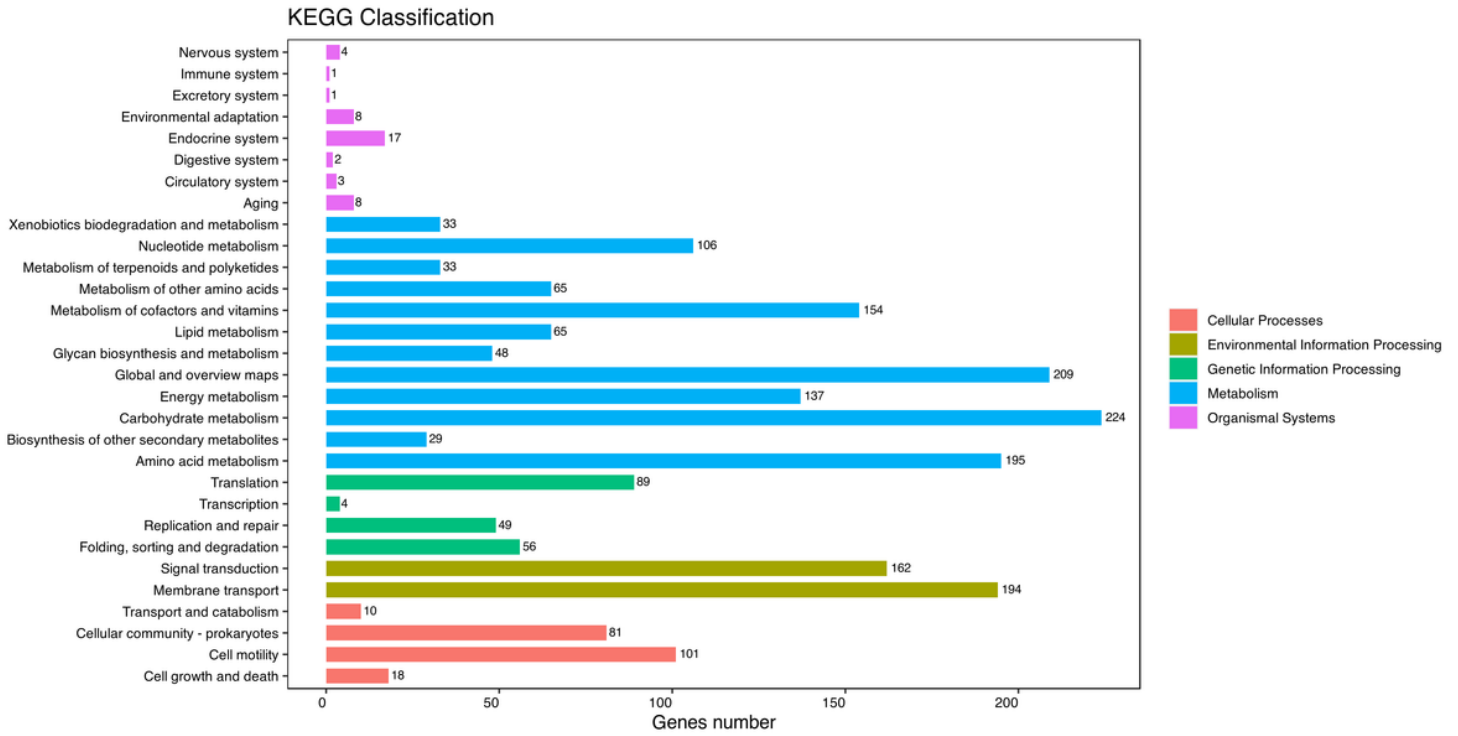


Figure 10

Gene distribution based on the Kyoto Encyclopedia of Genes and Genomes (KEGG) classification of *A. veronii* SJ4.

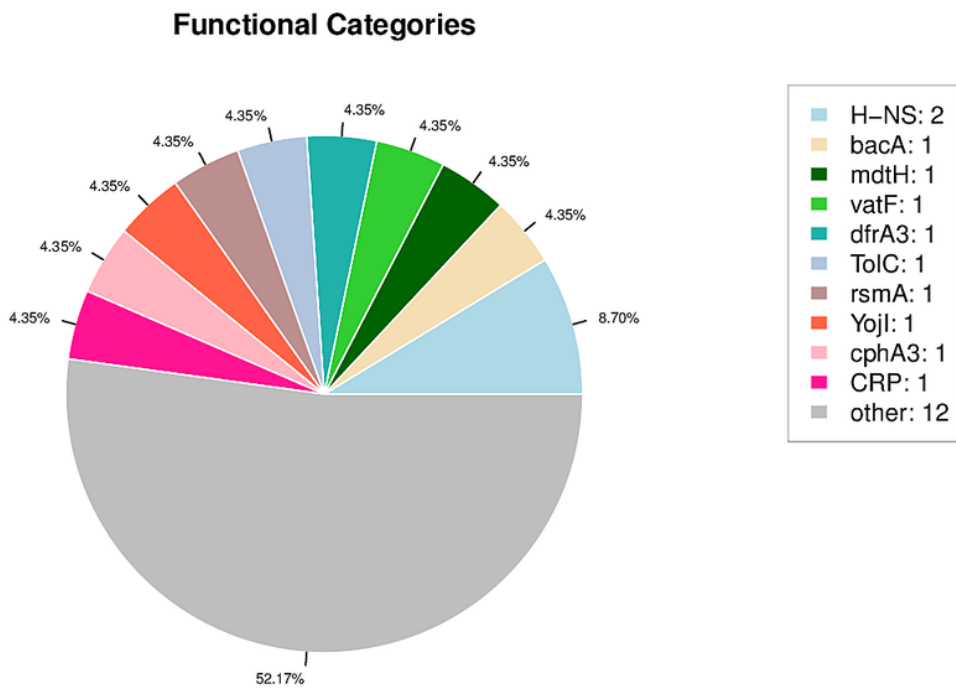


Figure 11

The top10 term display diagram among CARD database annotation. Note: The different sizes of fan-shaped sections in various colors indicate the proportion of genes annotated to the corresponding term, while the numbers following the legend located in the upper left corner represent the total number of genes annotated to the corresponding term.